Cenozoic provenance history of synorogenic conglomerates in western Argentina (Famatina belt): Implications for Central Andean foreland development

Federico M. Dávila[†]
Ricardo A. Astini[‡]
Centro de Investigaciones en Ciencias de la Tierra–Consejo Nacional de Investigaciones Científicas y Técnicas (CICTERRA-CONICET) and Laboratorio de Análisis de Cuencas, Universidad Nacional de Córdoba, Avenida Velez Sarsfield 1611, Córdoba X5016GCA, Argentina

ABSTRACT

In Famatina, at the modern northern flat-slab segment of the Central Andean belt, synorogenic conglomerate facies provide a unique opportunity to reconstruct paleogeography and tectonic setting. Stratigraphically constrained provenance analyses record a multievent history of the Andean foreland and a complex pattern of exhumed uplands, which, in turn, controlled the depocenter history. Western and eastern sources can be differentiated. The western domain was composed of equigranular granitoids and lower and upper Paleozoic volcano-sedimentary and sedimentary units, whereas the eastern domain was mainly formed by porphyrytic granitoids and minor slightly metamorphosed lower Paleozoic clastic rocks. The surrounding regions expose medium- to high-grade metamorphic rocks, which are not recorded in any Cenozoic conglomerate of Famatina. Unroofing sequences can be deduced from the compositional trends. Conglomerate composition and paleocurrent data show input from intrabasinal sources and important participation of basement since the beginning of the Neogene. We infer an early Miocene broken foreland during deposition of the Del Crestón Formation. A significant source inversion, with clasts supplied from the eastern basement domain, is recorded ~2000 m from the base, within the middle Miocene Del Abra Formation; reactivation of western granitic thrust sheets occurred by the late middle Miocene and late Miocene, as indicated by provenance studies of the Santo Domingo and El Durazno Formations. In contrast to simple asymmetric foreland models, provenance analysis documents early participation of crystalline rocks, suggesting early development of intraforeland basement highs within the southern Central Andes. At a regional scale, basement thrusting and associated intermontane basin development were diachronous. This interpretation is supported by broad propagation of basement thrusting from the northern Sierras Pampeanas (and Famatina) toward the central and eastern Sierras Pampeanas between early-middle Miocene and late Miocene–Pliocene time. Early Miocene reconstructions of the Juan Fernandez Ridge position on the Central Andean margin suggest that during this interval, shallow subduction was likely unrelated to oceanic plateau subduction under the Sierras Pampeanas.

Keywords: Central Andes, Sierras Pampeanas, broken foreland, basin analysis, provenance, conglomerates.

INTRODUCTION

East of the Central Andes along the modern flat-slab segment and ~500 km east of the Chile Trench, an intriguing basement foreland deformation system exists (Fig. 1); it is called the "Sierras Pampeanas broken foreland." This term refers to spatially isolated crystalline basement blocks that partitioned the foreland into a series of intermontane basins east of the high Andes (Jordan, 1995). The structural province is considered to be a modern analogue of the Late Cretaceous–Eocene Laramide (Rocky Mountain) province in the western United States (Jordan and Allmendinger, 1986). For both the ancient example and the modern analogue, foreland basement deformation has been linked to flat-slab subduction because of associated volcanism (ancient-modern), style of deformation (ancient-modern), and geophysical evidence (modern) that flat subduction was contemporaneous with the broken foreland deformation. In the Andes, however, neither the distribution of depocenters nor the timing of foreland partitioning is well known.

A key element of foreland basin fill is that its syntectonic nature records the unroofing history of related thrust systems (Graham et al., 1986; DeCelles, et al., 1987; Beck et al., 1988). Provenance studies on foreland strata provide information on both location and composition of adjacent source areas and on the pathways of transport from source to basin (Graham et al., 1975; DeCelles et al., 1993), regardless of factors that may influence the composition of sedimentary rocks (e.g., climate, geomorphology, and tectonics) (Haughton et al., 1991; Horton et al., 2002). Thus, time-constrained provenance data can aid in paleogeographic reconstructions, sequential restoration, and models for tectonic exhumation in adjacent uplands (e.g., Graham et al., 1986; DeCelles, 1994; among others).

Major spatial-temporal variations in retroarc strata have demonstrated that forelands behave nonuniformly as a result of along-strike variation in shortening history (e.g., Cardozo and Jordan, 2001), differential exhumation (e.g., Schlunegger, 1999), and/or paleoclimatic gradients (e.g., Horton, 1999). Provenance analysis can, therefore, be used as a tool to unravel these variations (e.g., Graham et al., 1986; DeCelles, 1988).

The aim of this work is to analyze the provenance history of Cenozoic conglomerates recorded in the Famatina broken foreland region of western Argentina. This area presents an outstanding opportunity to study the potential uplifted source terranes and the resultant proximal synorogenic deposits in a region where basement and stratigraphy can be accessed

[†]E-mail: fmdavila@efn.uncor.edu.
[‡]E-mail: raastini@efn.uncor.edu.

GSA Bulletin; May/June 2007; v. 119; no. 5/6; p. 609–622; doi: 10.1130/B26007.1; 9 figures; Data Repository item 2007087.

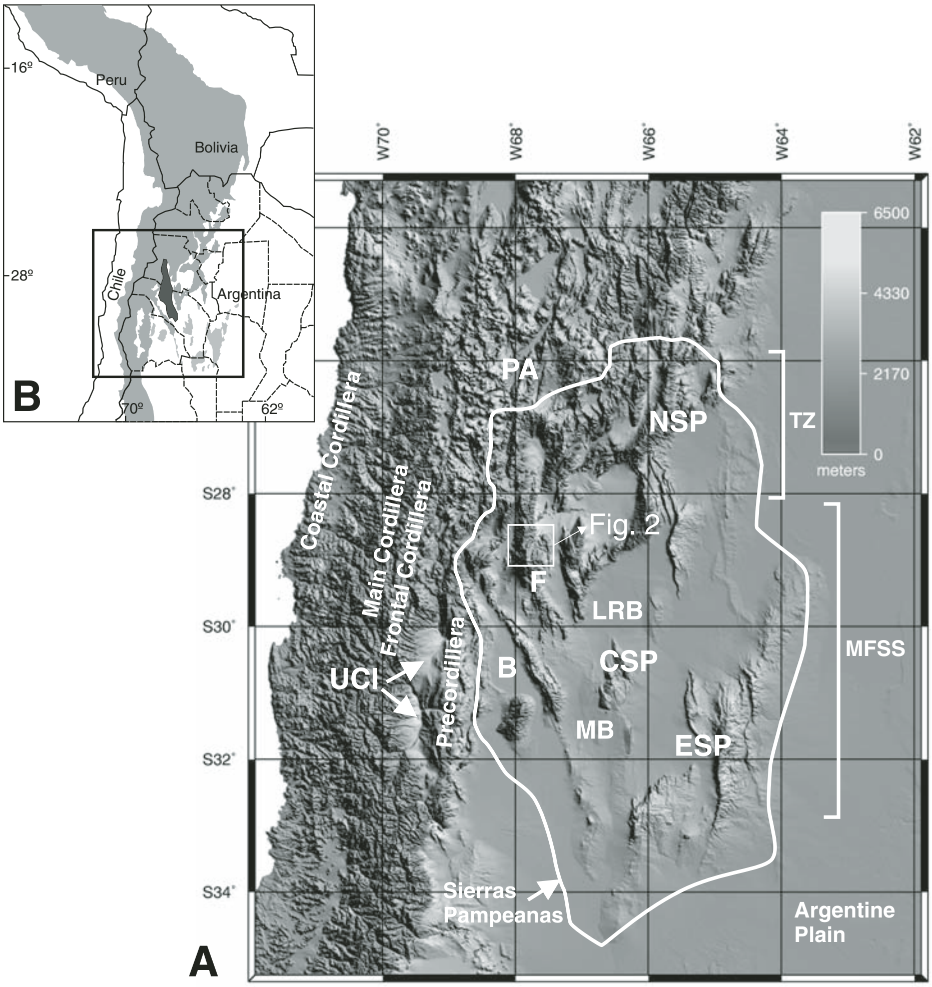

Figure 1. (A) Shaded topographic relief image (U.S. Geological Survey), showing: the Sierras Pampeanas (inside the white line) and its boundary regions (the Argentina Plain to the east and the Precordillera to the west). The Frontal Cordillera, Main Cordillera, Coastal Cordillera, and Puna Austral (PA) are shown for regional reference. The areas affected by modern flat-slab segment (MFSS) and transitional subduction zone (TZ) are shown (after Barazangi and Isacks, 1976). F—Famatina, B—Bermejo Basin, UCI—Calingasta-Uspallata-Iglesia basins, NSP—northern Sierras Pampeanas, CSP—central Sierras Pampeanas, ESP—eastern Sierras Pampeanas, LRB—La Rioja basin, MB—Mascasin basin. The white rectangle shows the location of Figure 2. (B) Map of the Central Andes (different gray tones), depicting (rectangle) the location of the shaded topographic relief image (A). The Famatina Range is shown for reference (darker gray). Country borders are shown by the dark lines, and the Argentina provinces are shown by dashed lines.

through several deep canyons in the rugged topography. Our results build upon recent contributions (e.g., Dávila and Astini, 2002, 2003a, 2003b; Dávila, 2003, 2005; Dávila et al., 2004a, 2004b), which allow us to determine foreland kinematics at this latitude that contrast with previous interpretations (e.g., Jordan et al., 2001; Ramos et al., 2002).

This analysis introduces new composition information and contributes to better understanding of the complex foreland evolution in the southern Central Andes. Four major aspects of the Andean foreland are discussed in this article: (1) the sharp along-strike variations of structural styles and complex paleogeography that control composition, (2) the protracted evolution of the NW Sierras Pampeanas broken foreland (Famatina belt) during the Andean cycle, (3) the timing of basement thrusting and its migration from north to south through the Neogene, and (4) a novel early Miocene flat-slab subduction episode, with foreland partitioning, not linked to the Juan Fernandez ridge collision. The latter point is of particular interest for geodynamic reconstructions because Miocene to Holocene flat-slab subduction in the Central Andes has been closely tied to southward migration of the Juan Fernandez aseismic ridge (see Yañez et al., 2001; Kay and Mpodozis, 2002). Our data introduce strong arguments against that hypothesis, at least for the early and middle Miocene.

GEOLOGIC SETTING AND CENOZOIC STRATIGRAPHY

This work focuses on the flat-slab segment (cf. Barazangi and Isacks, 1976) of the southern Central Andes (28°–33°S), where the Nazca plate descends at low angle under South America, causing broadly distributed seismologic activity and obliterating volcanism. In this segment, four main Andean belts are recognized from west to east (Fig. 1): the Coastal Cordillera in the present Chilean forearc; the Main Cordillera along the Chilean-Argentine border; the thin-skinned fold-and-thrust belt of the Precordillera, and the basement-involved Sierras Pampeanas region (the broken foreland). Jordan et al. (2001, p. 794) differentiated three evolutionary stages along this broad segment: (1) an asymmetric “wedge-like simple foreland” between 20 and 7.3 Ma, (2) a “symmetrical foreland basin” between 7.3 and 6.5 Ma, and (3) a “broken foreland” between 6.5 Ma and present. The latest stage is frequently linked to the evolution of the intraforeland Sierras Pampeanas, where crustal-scale thick-skinned thrusts affected depocenter distribution. The Bermejo Valley (B in Fig. 1) separates the thin-skinned wedge-top (east-vergent fold-and-thrust belt) from the broken foreland and serves as a major longitudinal sediment storage region.

The Famatina belt extends for ~400 km between 27° and 31°S (Fig. 1, inset) in La Rioja province, western Argentina. It is located between the Bermejo Valley and the Sierras Pampeanas region (Fig. 1). Despite its position in the foreland, at >500 km from the trench, altitudes are over 6000 m. Its structure has variously been interpreted as doubly vergent, high-angle, basement thrusts (see Dávila and Astini, 2002, 2003b; Ramos et al., 2002; Dávila et al., 2003, 2004a). Two major doubly vergent basement uplifts bound the Angulos-Famatina Valley (the Cordón de la Cumbre to the west and the Sierra de Paimán–Ramblones to the east), where there are several thousand meters of accumulated Cenozoic strata (Fig. 2). Paleozoic strata (e.g., Dávila, 2003; Dávila et al., 2003) crop out in various thrust sheets in the study area (Fig. 2).

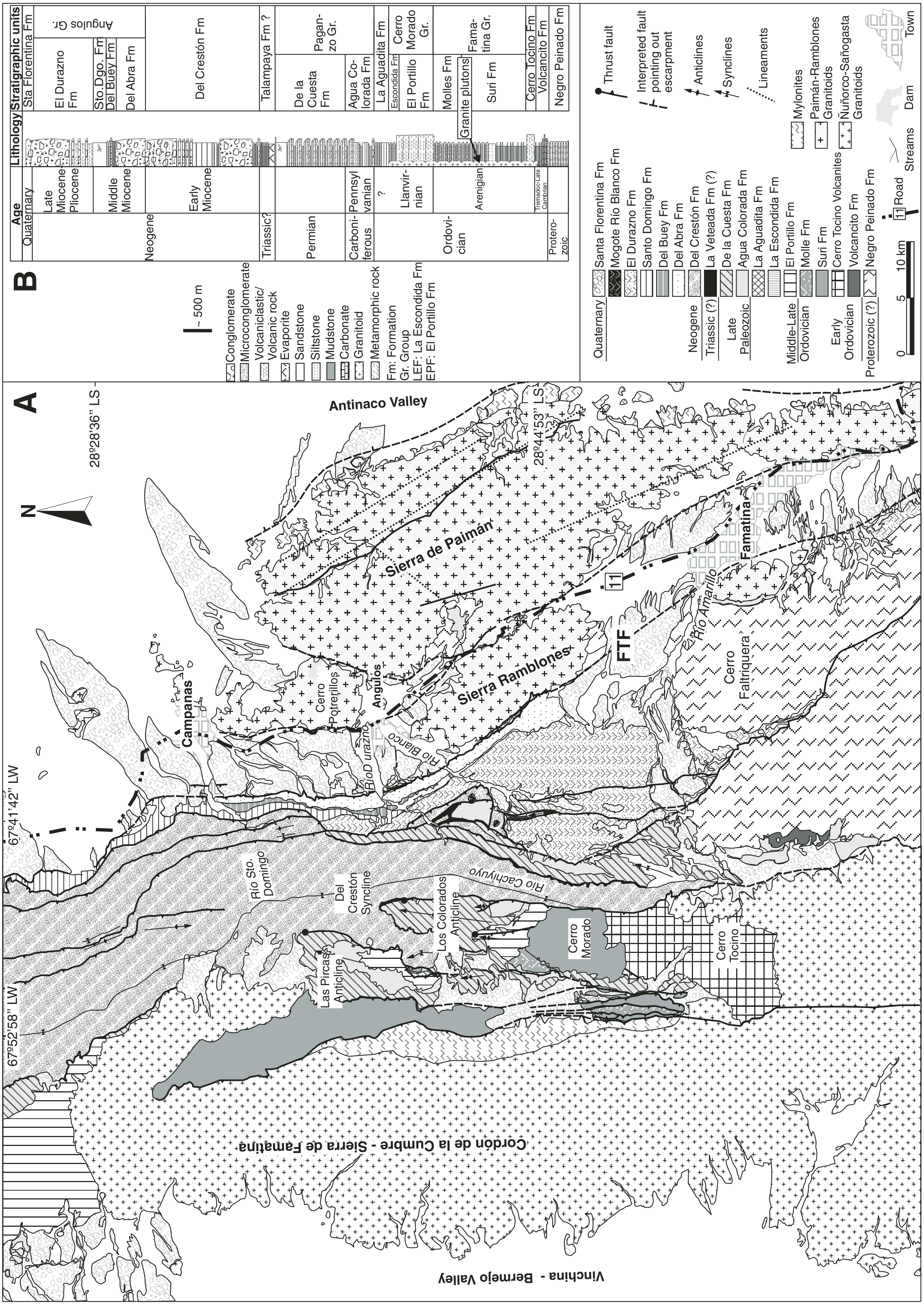

Figure 2. (A) Geologic map of the central Famatina belt (after Dávila, 2003) showing the main source domains. (B) Stratigraphic column for the Famatina area. FTF—Famatina thrust front.

Figure 3. Synthetic stratigraphic column, showing from left to right, the Tertiary synorogenic strata of Famatina and the maximum conglomerate clast sizes along with upward-coarsening (UC) and upward-fining (UF) trends of megasequences (MS) (black bars next to maximum clast size column). Conglomerate composition (*n* = 27,000) is shown in the third column by the pie charts, depicting the mean percentages of involved source lithologies (see details in Appendix 3, see text footnote 1). Paleocurrents (*n* = 166), in the right column (arrows), are measured from imbrications and cross-stratifications (see details in Fig. 5). Numbers in parentheses, next to the composition pie charts, correspond to those depicted in the Appendix 3 (see text footnote 1) and characterize the different analyzed sections.

Cenozoic Stratigraphy

The Del Crestón Formation, the overlying Angulos Group, and the Santa Florentina Formation record the complete synorogenic Cenozoic history within the eastern slope of the Famatina Ranges (Figs. 2 and 3). These >3500-m-thick alluvial strata are arranged into six continental megasequences (Fig. 3), represented from bottom to top by: (1) the lower section of the early Miocene Del Crestón Formation (ca. 17–16 Ma, MS 1), (2) the upper section of the Del Crestón Formation (MS 2), (3) the early middle Miocene Del Abra Formation and lower part of the middle Miocene Del Buey Formation (MS 3), (4) the upper part of the middle Miocene Del Buey (MS 4) and Santo Domingo Formations (MS 4), (5) the late Miocene–early Pliocene El Durazno Formation (MS 5), and (6) the Pliocene–Pleistocene Santa Florentina Formation. The youngest Pliocene-Pleistocene megasequence is not included in this work, because its depositional systems and paleocurrents are related to a tectonic landscape comparable to the present-day situation.

The Del Crestón Formation MS1 unconformably overlies Permian (-Triassic?) red beds. Recent ^{40}Ar-^{39}Ar dating on andesite boulders at the base of the unit yields an early Miocene age (17–16 Ma; Dávila et al., 2004b). Two major upward-thickening and -coarsening sequences compose this 1800-m-thick sedimentary succession, MS1 and MS2 (Dávila and Astini, 2002). The lower megasequence MS 1 (Fig. 3) is composed of a distinct, thin, sheet-like, fine-grained conglomerate (Fig. 4A) overlain by fine-grained deposits of saline playa lakes and by ~450 m of andesite-rich coarse conglomerates (Fig. 4B), which are interpreted as proximal debris-flow–dominated alluvial-fan deposits. Dávila et al. (2004b) interpreted these deposits as lahar sequences. Fine-grained red beds initiate the second upward-thickening and -coarsening megasequence MS 2 (Fig. 3). Sandy polymictic conglomerates become more common and thicker upsection. These, in turn, are capped by a 370 m, coarse, granite-rich conglomerate (Figs. 4C and 4D), which is interpreted to be related to prograding, stream-dominated megafans (Dávila and Astini, 2002; Fig. 4C).

The Angulos Group (Dávila, 2005) is 1942 m thick and is represented from bottom to top by the Del Abra MS3 (505 m), Del Buey (348 m) upper MS3–lower MS4, Santo Domingo MS4 (213 m), and El Durazno MS5 (876 m) Formations. Late Miocene–Pliocene ages (6.9 ± 1.2 Ma and 4.0 ± 0.8 Ma; Tabbutt, 1990) were originally considered to encompass all synorogenic strata in the Famatina region. However, recent studies have demonstrated that they only constrain the uppermost section of the Angulos Group (Dávila, 2005). These three megasequences (MS3 to MS5) record a complex middle Miocene to Pliocene foreland evolution within the Famatina belt.

The upward-thinning-fining cycle MS3 of the Del Abra Formation (Fig. 4E), with granite megaboulders in its base, has been interpreted as related to mid-Miocene normal faulting (see details in Dávila and Astini, 2003a). The Del Buey Formation, top of MS3 and base of MS4 (Fig. 3), is a dominantly fine-grained aggradational succession interbedded with fluvial granulate conglomerates (Fig. 4F) and paleosols and laterally continuous stromatolite-rich, fossiliferous carbonates (Fig. 3; see also Dávila and Astini, 2003a). This interval shows a period of basin starvation prior to initiation of major sediment and tectonic loading. The *Corbícula stelzneri* bivalves in carbonate intervals (Turner, 1971), correlated laterally with ca. 14 Ma Paranaense marine beds (Bossi et al., 2002; Hernández et al., 2005), together with palynological studies (Barreda et al., 2006) on yellowish to greenish siltstone horizons, indicate a middle Miocene age for the Del Buey Formation top MS3–lower MS4. The boundary with the eolian-dominated Santo Domingo Formation upper MS4 is represented by a short interval of braided-stream conglomerates and interbedded eolian sandstones (Dávila, 2005). The progradation of this fluvial-eolian succession, together with the uppermost section of the Del Buey Formation, constitutes the fourth upward-coarsening megasequence MS4. The El Durazno Formation overlaps the Santo Domingo Formation upper MS4 above a major erosional surface and comprises the fifth upward-thickening and -coarsening megasequence MS5, which is punctuated by pyroclastic-flow deposits (Martina et al., 2006; Fig. 4G). The first laterally continuous ignimbrite bed is ~1000 m above the base of the Angulos Group (Fig. 3). This is the oldest tuff dated by Tabbutt (1990), according to the stratigraphic position, and this is supported by our own ^{40}Ar-^{39}Ar isochron ages of 5.2 ± 0.85 Ma (see Appendixes 1 and 2[1]). Toward the top of the El Durazno Formation, the unit progressively coarsens up into sandy cobble conglomerate (Fig. 4H) and shows deep (>1 m) cut-and-fill structures, indicating unstable braided-fluvial systems and stream-dominated alluvial-fan environments (Fig. 3).

In the Río Blanco region (Fig. 2), two undated porphyritic dacite domes (Mogote Cerro Blanco and the Cerrito Blanco) intrude Lower Miocene rocks but would have supplied dacite fragments during sedimentation of the Durazno Formation. Preliminary provenance studies (Martina et al., 2006) together with stratigraphic and structural relationships (Dávila et al., 2004a) suggest that the domes formed post–early Pliocene to Pleistocene.

The youngest synorogenic unit in Famatina is the Pliocene–Pleistocene Santa Florentina Formation (Lencinas, 1994) (Fig. 3). This unit forms the higher alluvial terraces and overlies older formations (Paleozoic to Pliocene) above an erosional, locally angular, discordance. The sedimentological features of the Santa Florentina Formation, analogous to the lowermost terraces, allowed us to compare similar depositional systems and surface gradients to those developing at present and draining eastward from the Cordón de la Cumbre (Fig. 2). The last major Andean rejuvenation and episode of deformation in the region took place in Pliocene–Pleistocene times based on rotation of strath and fill terraces and thrusting and fault scarps involving the terraces. High-gradient Holocene colluvium and alluvial fans presently developing within the region form the uppermost level of terraces and unconformably overlie the Santa Florentina Formation.

POTENTIAL SOURCE AREAS

Potential sources within the central Famatina region can be separated into two contrasting domains on the basis of the composition of

[1]GSA Data Repository item 2007087, Appendixes 1–3, is available on the Web at http://www.geosociety.org/pubs/ft2007.htm. Requests may also be sent to editing@geosociety.org.

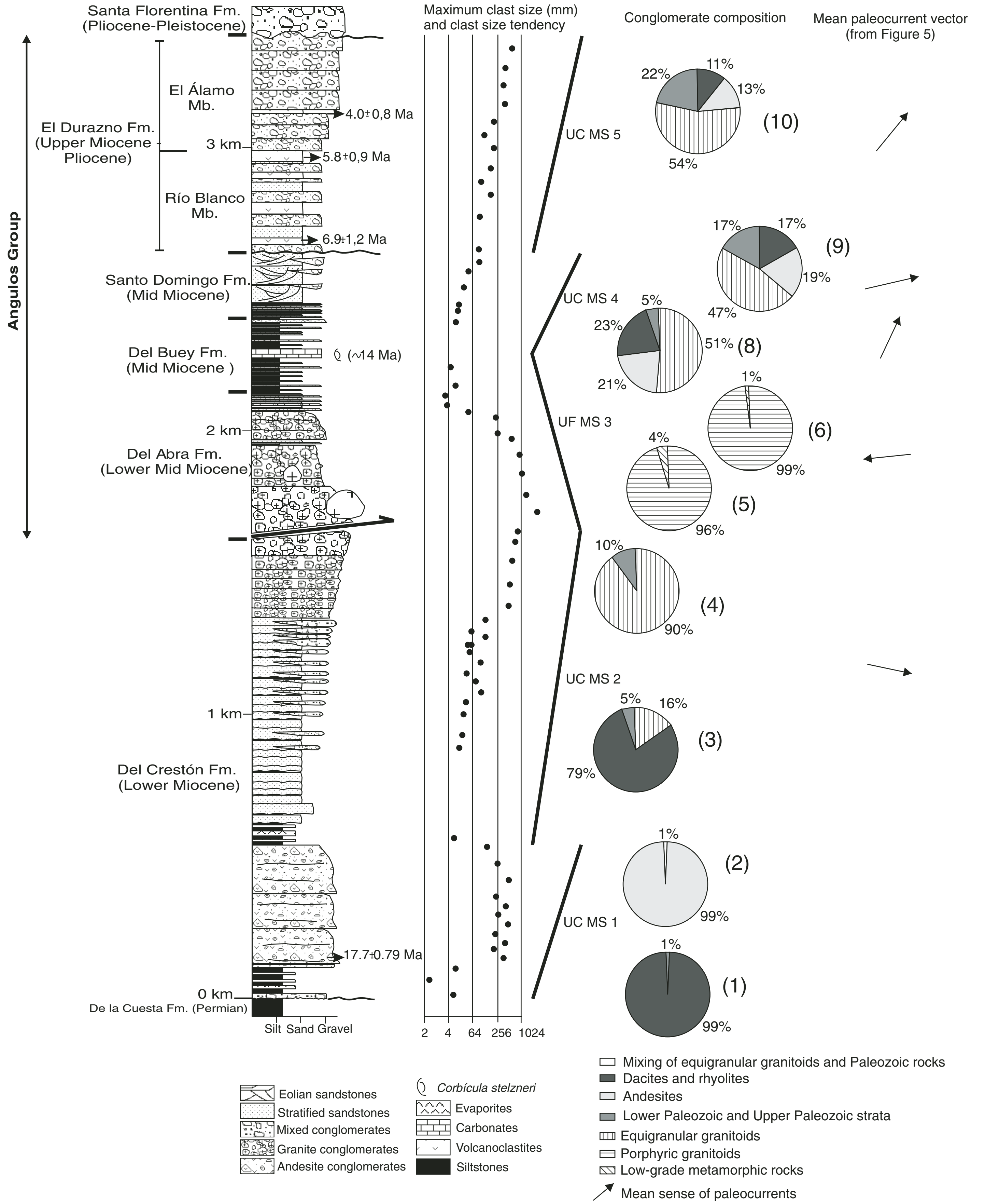

Santa Florentina Fm.
(Pliocene-Pleistocene)
El Álamo Mb.
El Durazno Fm.
(Upper Miocene Pliocene)
Río Blanco Mb.
Santo Domingo Fm.
(Mid Miocene)
Del Buey Fm.
(Mid Miocene)
Del Abra Fm.
(Lower Mid Miocene)
Del Crestón Fm.
(Lower Miocene)
De la Cuesta Fm. (Permian)
Angulos Group
3 km
2 km
1 km
0 km
4.0± 0,8 Ma
5.8 ±0,9 Ma
6.9±1,2 Ma
(~14 Ma)
17.7±0.79 Ma
Silt Sand Gravel
Maximum clast size (mm) and clast size tendency
2 4 64 256 1024
UC MS 5
UC MS 4
UF MS 3
UC MS 2
UC MS 1
Conglomerate composition
Mean paleocurrent vector (from Figure 5)
(10) 22% 11% 13% 54%
(9) 17% 17% 19% 47%
(8) 5% 23% 51% 21%
(6) 1% 99%
(5) 4% 96%
(4) 10% 90%
(3) 5% 16% 79%
(2) 1% 99%
(1) 1% 99%
Eolian sandstones
Stratified sandstones
Mixed conglomerates
Granite conglomerates
Andesite conglomerates
Corbícula stelzneri
Evaporites
Carbonates
Volcanoclastites
Siltstones
Mixing of equigranular granitoids and Paleozoic rocks
Dacites and rhyolites
Andesites
Lower Paleozoic and Upper Paleozoic strata
Equigranular granitoids
Porphyric granitoids
Low-grade metamorphic rocks
Mean sense of paleocurrents

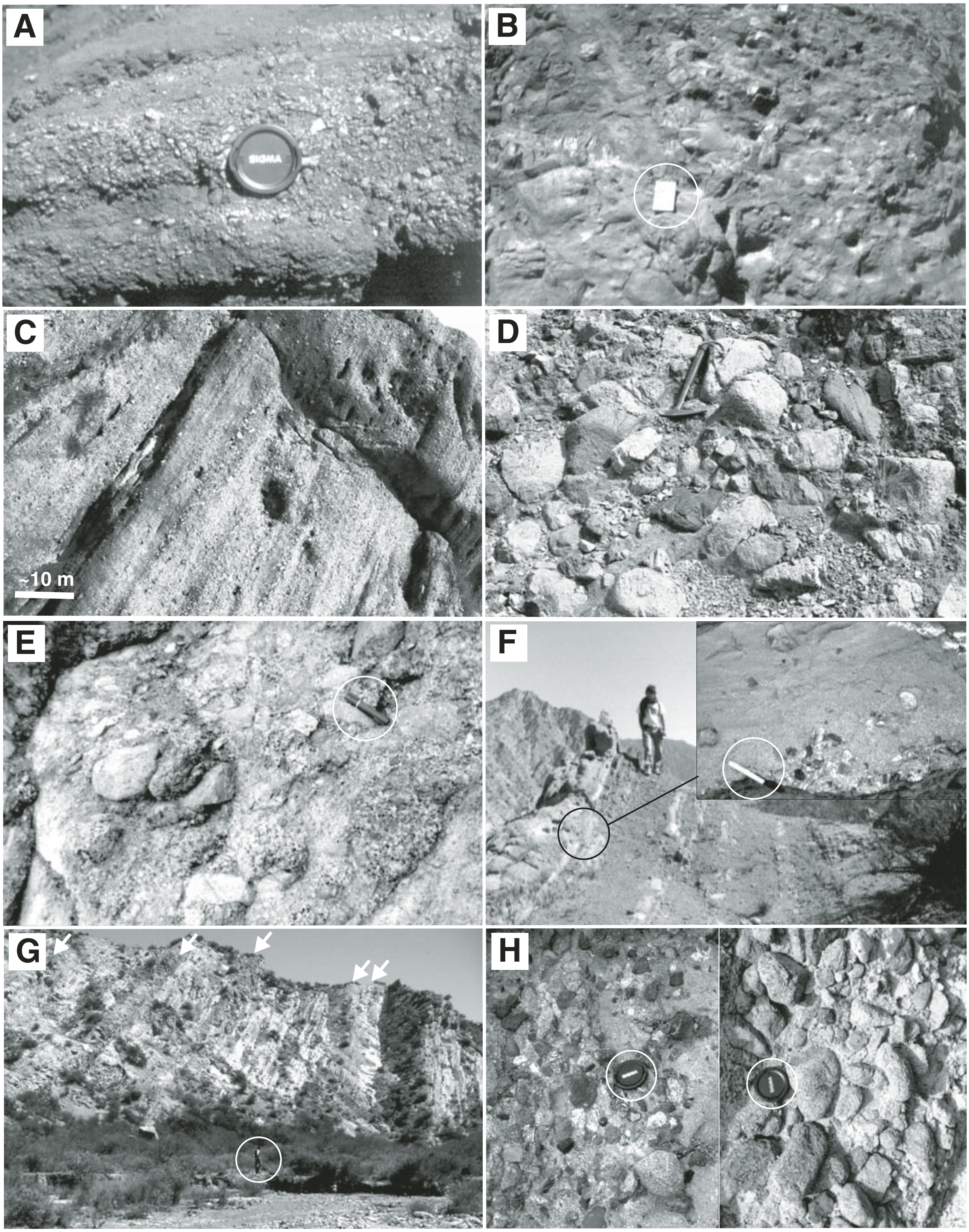

Figure 4. Textures and fabrics of synorogenic conglomerates of Famatina. (A) Basal microconglomerate of Del Crestón Formation. (B) Andesite conglomerates of lower megasequence MS1 of Del Crestón Formation. (C–D) Equigranular granite-rich conglomerate at top of the second megasequence MS2 of Del Crestón Formation. (E) Porphyritic granite-rich conglomerate in lower megasequence MS3, Del Abra Formation. (F) Pebbly conglomerates in lower megasequence MS4, Del Buey Formation (upper section). (G) Thick volcaniclastic succession interlayered with clastic conglomerate in MS5, lower section of El Durazno Formation. White arrows depict ignimbrites. (H) Large cobble polymictic conglomerate in the upper section of MS5, El Durazno Formation (left), and granite conglomerates, locally mixed with rhyolite, dacite, and andesite clasts (darker clasts) in uppermost section of MS5, El Durazno Formation (right).

major basement uplifts and overlying stratigraphy. Presence or absence of certain lithologies may be used as a first-order discriminator of source areas.

Porphyritic coarse-grain two-mica granites and monzogranites with major mylonite zones and a localized low-grade metamorphic sedimentary cover constitute the eastern domain (Fig. 2) along the Sierra de Paimán–Ramblones (Dávila, 2003).

Exposures along the Cordón de la Cumbre and within the Famatina thrust belt constitute the western domain (Fig. 2). The granitoids along the Cordón de la Cumbre lack big feldspar porphyroclasts and include partly mylonitized, equigranular granodiorites, monzogranites, and tonalites of medium to coarse grain size (>500-m-thick shear zone) (Astini and Dávila, 2004). The western domain basement is covered by a thick (>4500 m) Paleozoic cover, and it is flanked by Cenozoic synorogenic strata (>4000 m) (Dávila et al., 2004a) (Fig. 2B). These sequences constitute the east-vergent fold belt of Famatina. Paleozoic rocks are Lower Ordovician deep-marine sedimentary and shallow-marine volcano-sedimentary successions (Famatina Group), Middle Ordovician rhyolites and volcano-sedimentary rocks (Cerro Morado Group), Pennsylvanian coarse whitish-to-yellowish arkoses with green silty shales and intervals of black carbonaceous shales (Agua Colorada Formation), and Permian conglomerates and red beds (De La Cuesta Formation).

Lower Cambrian medium- to high-grade metamorphic rocks pervasively intruded by Ordovician granites surround the Famatina belt, unconformably covered by upper Paleozoic red beds. Outcrops of metasedimentary rocks in greenschist facies have patchy exposures in the region. Several mylonite zones affecting granites (e.g., Höckenreiner et al., 2003) also developed within these ranges. A relatively thin sliver of Grenville-age basement rocks separates it from the Precordillera thin-skinned thrust belt region (Fig. 1). Amphibolites, schists, gneisses, crystalline marbles, and migmatites characterize these medium- to high-grade metamorphic ranges, intruded by a few granite bodies (mostly pegmatites) and a >1000-m-thick upper Paleozoic sedimentary cover (Caminos, 1979a). Farther west, in the Cordilleran regions, Permian-Triassic granites dominate, with subordinate coeval rhyolites (Caminos, 1979b).

METHODS

Conglomerates usually represent the least-recycled detritus from a source area (Graham et al., 1991). Complex source terrains preclude detailed provenance modeling (e.g., DeCelles, 1988). We complemented the compositional analysis of conglomeratic deposits with paleocurrent data. The composition analysis was based on systematic field counting using square-meter grids for boulder-cobble conglomerates and quarter-square-meter grids for finer-grained conglomerates. Along 10 cm equidistant parallel lines within each grid, we measured the various compositional lengths per line. Compositional lengths were added and converted into percentages. An average of 100 clasts per grid was counted for coarse conglomerates (>64 mm); for medium- (32–64 mm) and fine-grained (2–32 mm) conglomerates, this number increased. A minimum of 30 grids within each conglomeratic sequence assured statistically representative counted clasts. Maximum-clast-size plots in Figure 3 were calculated using the method of Surlyk (1978). Compositional data are summarized in Appendix 3 (see footnote 1), showing percentages of lithologies throughout the synorogenic succession (Fig. 3).

For paleocurrents, collection and analysis of directional structures followed Graham (1988, and references therein). The bulk of the data, on fluvial beds, was collected from imbricate clasts [a(t)-b(i)] and the rest from trough cross-bedding. Additional measurements were taken from channel-axis orientation and unidirectional ripple marks to complement other information. The eolian beds were sampled on foresets of mega-cross-stratified beds. Measurements were plotted on current rose diagrams.

CONGLOMERATE COMPOSITION AND CALIBER

Clast composition is summarized in Appendix 3 (see footnote 1) and variations in the Cenozoic stratigraphy of Famatina are depicted in Figure 3.

Del Crestón Formation

The base of the Del Crestón Formation (base of MS1, 1 in Appendix 3 and Fig. 4A) shows lithologies comparable to the volcanic Ordovician unit exposed within the Cerro Tocino and the Cerro Morado (Fig. 2). The small amount of reddish silty sandstone clasts indicates exhumation of Permian red beds. The upper 273 m of megasequence MS1 (2 in Appendix 3 and Fig. 4B) consist almost totally of andesite boulders up to 0.6 m, which provide a ca. 17 Ma crystallization age (Dávila et al., 2004b). Trace amounts of Ordovician, Pennsylvanian, and Permian sedimentary sources and equigranular granitoids indicate exhumation of the Cordon de la Cumbre thrust sheet. The uppermost megasequence of the Del Crestón Formation MS2 (3 in Appendix 3) is characterized by a short interval with plutonic and sedimentary clasts. Multistory red sandstones with local lags of mud chips and boulders dominate the lower section of MS2 (see Fig. 3). Sandstones are lithic-rich (Dávila and Astini, 2002); lithics are represented by various volcanic, sedimentary, and granite fragments. The scarcity of gravel sheets in this part of the section may relate to a low gradient within the alluvial setting and/or with intense weathering of upper Paleozoic strata in the source area. Carboniferous arkoses and Permian red beds are highly erodible in comparison to lower Paleozoic rocks. We infer that source disaggregation could have been favored by wetter climate conditions, as inferred from lithofacies analysis in these fluvial strata (Dávila and Astini, 2002). The oldest extraformational conglomerate in MS2 at ~300 m is an ~150-m-thick interval dominated by Paleozoic sandstones clasts, with minor rhyolites and equigranular granitoids (see 3 bottom in Appendix 3). Immediately on top of this interval (see 3 top in Appendix 3), clasts are mostly represented by felsic volcanic rocks and equigranular granitoids, with minor Paleozoic sedimentary rocks. The uppermost section of MS2 (see Fig. 4C) is a transition to a boulder granite-rich conglomerate (size range between 0.1 and 1 m), dominated by equigranular granite clasts.

Del Abra Formation

Conglomerates in the Del Abra Formation (MS3) are coarse and compositionally homogeneous. Granite cobbles and boulders are of the porphyric granitoid type (Appendix 3 [see footnote 1]; Figs. 3 and 4E) and are comparable to those exposed in the Sierra Paimán–Ramblones. Low-grade metamorphic rocks and mylonites decrease from bottom to top of the formation (compare 5 and 6 in Appendix 3). Metasedimentary rocks are also like those in patchy exposures along the Sierra de Paimán–Ramblones (Astini et al., 2005).

Del Buey Formation

This unit is composed of a few fine-grained conglomerate sheets (50–150 mm). Their composition is dominated by volcanic and plutonic clasts, with minor amounts of sedimentary clasts (see Appendix 3 [see footnote 1]; Fig. 4F). Toward the base, porphyric granitoid clasts dominate (uppermost MS 3, see 7 in Appendix 3) similar to those exposed in the Sierras de Paimán–Ramblones, whereas the upper section (lowermost MS4) is entirely formed by equigranular granitoid fragments (see 8 in Appendix 3; Fig. 3) like those exposed in the core of the Famatina thrust belt. Volcanic pebbles in the upper section are andesites comparable to those in the megasequence MS1 (lower Del Crestón Formation), plus some felsic volcanic rocks. Low-grade metamorphic rocks are not present toward the top of the unit (see Appendix 3). Sandstones clasts were derived from Paleozoic strata (see Appendix 3).

Santo Domingo Formation

Conglomerates in this unit (upper MS4) contain polymictic cobbles to boulders (0.1 m, Fig. 3). Mean clast composition (9 in Appendix 3) is characterized mostly by equigranular granite fragments and volcanic clasts derived from the Famatina thrust belt. Sedimentary clasts are upper Paleozoic white and red sandstones and Ordovician silicified green sandstones and black shales. Arkosic composition of interbedded eolian sandstone sheets is compatible with conglomerate composition (Dávila and Astini, 2003c). Sand grains are 30% quartz, 30% rock fragments (mostly granite grains) and 40% feldspar (20% potassium feldspar and 20% plagioclases).

El Durazno Formation

The conglomerate composition of the El Durazno Formation (MS5) is very similar to the Santo Domingo Formation (upper MS4). These two units, however, do not constitute a single sedimentary cycle, as indicated by the regional unconformity that separates MS4 from MS5 (Fig. 3). With respect to the upper MS4, MS5 shows a significant increase in clast size (maximum mean clast size 0.3 m; Figs. 4F and 4G), with boulders locally over 1 m. Two interesting features in this megasequence are the presence of a few laminated limestone cobbles and channel-lag deposits, with >99% porphyric dacite clasts. The rich volcanic composition corresponds to the Rio Blanco Member, which is distinguished from the rest of MS5 by interlayered ignimbrites (Fig. 4G) (Martina et al., 2006).

PALEOCURRENT DATA

The Del Crestón Formation has few paleocurrent indicators in MS1, but excellent indicators in MS2 (see Fig. 5). MS1 preserves a few imbricated and clustered clasts within the hyperconcentrated-flow deposits that locally intercalate debris-flow sheets (Dávila and Astini, 2002). The paleoflow pattern in these beds is polymodal. In contrast, the Del Crestón Formation MS2, constituted mostly by imbricated clasts and fluvial cross-beds, exhibits paleocurrents to the east (Fig. 5).

From bottom to top, the base of MS3 (lenticular conglomerates of the Del Abra Formation) shows west-directed paleoflows (Fig. 5), measured from imbricated clasts and trough cross-beds.

The few data collected on the top of MS3 (basal section of Del Buey Formation) show westward paleocurrents consistent with measurements on top of the upper gradational boundary with the Del Abra Formation (also top of MS3). Most paleocurrent data were collected on the uppermost part of the Del Buey Formation (base of MS4) from cross-stratified beds and only a few from imbricated conglomerates. Paleocurrent distribution in the base of MS4 shows a polymodal pattern (Fig. 5).

The dominant eolian strata of the Santo Domingo Formation (top of MS4) were analyzed independently from the interbedded braided-fluvial packages. Paleowinds flowed toward the SSW (see Dávila and Astini, 2003c). Paleocurrents in the fluvial conglomeratic facies show a unimodal pattern with a mean vector to the east (see Fig. 5).

The fluvial imbricated conglomerates of MS5 indicate a unimodal distribution of paleocurrents to the NE (see base and top sections diagrams in Fig. 5).

RECURRENT BASEMENT UNROOFING FROM PROVENANCE ANALYSIS

Provenance analysis, together with sedimentologic and stratigraphic studies, demonstrates that Cenozoic sedimentation in Famatina occurred within proximal alluvial environments, strongly influenced by unroofing of nearby crystalline source areas. The entire synorogenic succession indicates a local provenance history, with no input from inner (hinterland) Cordilleran regions or from eastward cratonic sources. The succession of clast compositions and associated paleocurrents can be related to the exhumation of the two domains presently recognized in the central region of the Famatina ranges. Changes in the local source area indicate deformation of separate basement highs across the region, demonstrating that the foreland basin in the area has been broken into basement core uplifts since the beginning of the Andean cycle.

1. Early Miocene (Del Crestón Formation, MS1 and MS2)

Compositional and paleocurrent information indicates that the main source of Lower Miocene Del Crestón Formation clasts was the western domain, consisting of the crystalline block of the Cordon de la Cumbre and the Famatina thrust front (FTF in Fig. 2). Clasts are mostly first order, cycling from volcanic terrains and crystalline sources (Figs. 3 and 6), as suggested by clast sizes. Underlying Paleozoic units do not contain boulders as large as those recorded in Cenozoic strata. Fine grain size and felsic volcanic composition suggest that recycling may have occurred only in the basal sheet-like microconglomerate of the Del Crestón Formation (Dávila and Astini, 2002). Although no felsic volcanic sources are documented to the east of the Famatina belt, to the west, potential source areas are the Triassic volcanic sequences in the Frontal Cordillera (Fig. 1) (e.g., Choiyoi Group; see Caminos, 1979b) and the Ordovician Cerro Tocino and Cerro Morado volcanics, which are exposed immediately west of the Cenozoic exposures (Fig. 2).

The andesite boulders of the lower megasequence MS1 (Fig. 3) suggest derivation from a volcanic landscape. Regardless of the precise volcanic source location (see Dávila et al., 2004b), low clast variability suggests that either bulk rock exposure in the source area did not change significantly or changes were buffered within the drainage network (e.g., Steidtmann and Schmitt, 1988). The presence of outsized andesite boulders, plagioclase-rich matrices, and gravity-flow deposits (lahars) suggests a close volcanic source (Dávila and Astini, 2002; Dávila et al., 2004b). Only at the top of MS1 do some granite pebbles occur, indicating dilution. A bimodal paleocurrent pattern (Fig. 5) indicates periodic changes in the stream network of the region, possibly related to volcanic deposition. The sedimentary package geometry, with apex to the west, and clast size reduction toward the east, may indicate an eastward-tilted paleosurface. This is supported by similarly oriented rotational unconformities (Dávila and Astini, 2003b), which suggest a local volcanic source toward the west. Polymodal paleocurrent patterns point to multiple sources.

Provenance of the next upward-coarsening megasequence MS2 (Fig. 3) represents a complete unroofing megasequence sourced from the west (Fig. 7). Paleocurrent patterns support this interpretation. A high proportion of unequivocal Cordon de la Cumbre–derived granite clasts at the top of this megasequence suggests erosion of deeper levels during later stages of unroofing. A plot of clast compositional ratio versus stratigraphic level (Fig. 6) shows plutonic sources fully exposed by the end of MS2 deposition. The inverted compositional trend of MS2 with respect to the local stratigraphy (compare Figs. 2 and 3) is that of a typical unroofing sequence (Colombo, 1994), derived from removal of intrabasinal Paleozoic sources. The unroofing trend ends with crystalline basement exhumation, as reflected by the granitic conglomerates at the top (Fig. 3).

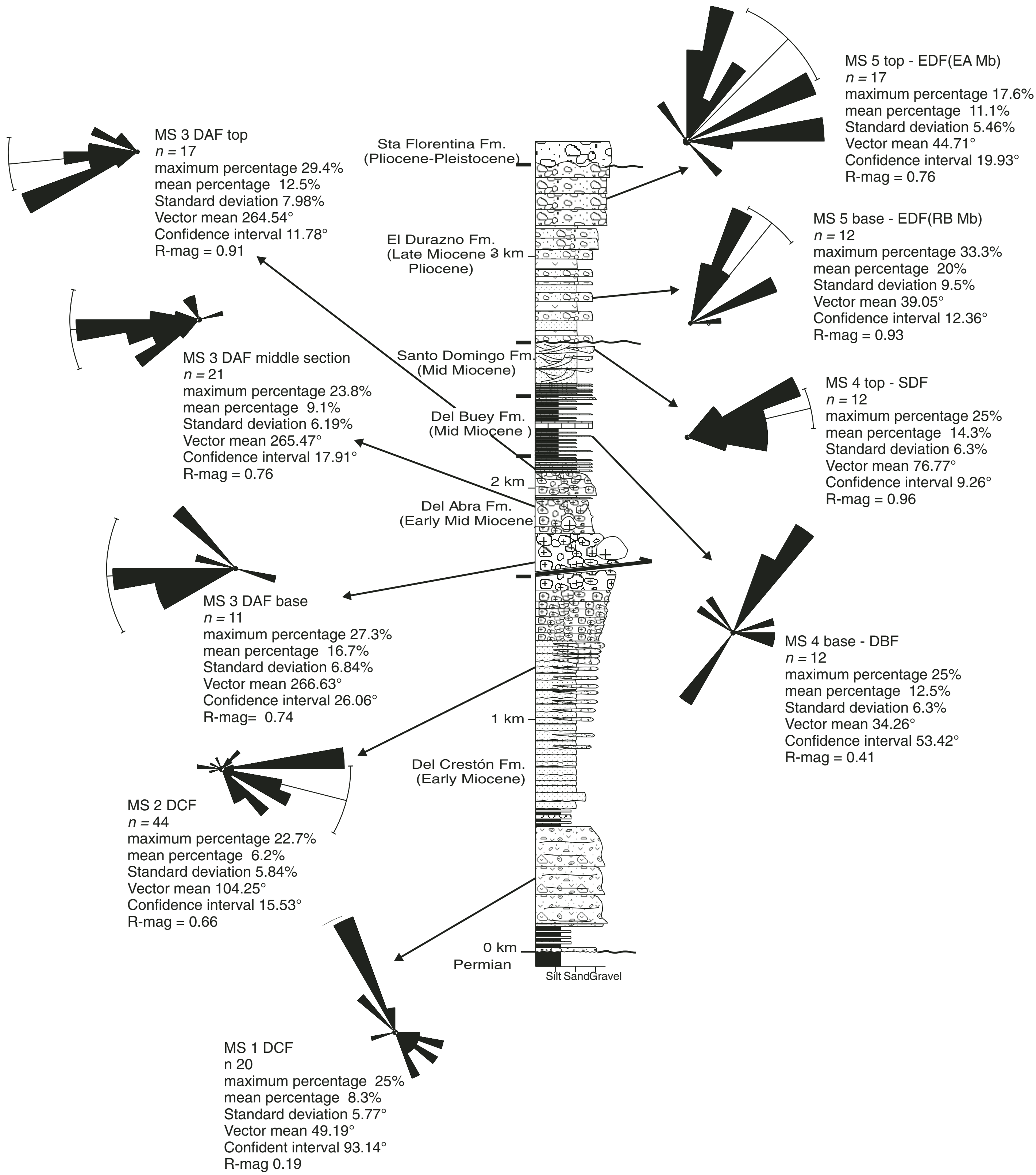

Figure 5. Paleocurrent roses of synorogenic conglomerates, eastern side of Famatina Ranges. Roses are plotted at 10° class interval.

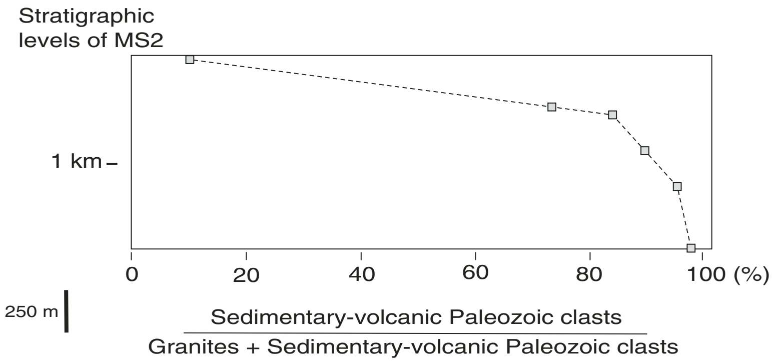

Figure 6. Plot of clast compositional ratio for the Lower Miocene Del Crestón Formation relative to stratigraphic levels, showing temporal variation in clast composition in megasequence MS2. Note increasing granite composition upsection, indicating basement unroofing.

Basin Implications

Unroofing of granites and mylonite belts in the Sierra de Famatina indicates that thrusting of crystalline basement occurred in the western Sierras Pampeanas region as early as early Miocene (Figs. 7 and 8). This indicates that the retroarc region was partitioned, in contrast to previous interpretations of a simple asymmetric foreland (e.g., Jordan et al., 2001; Ramos et al., 2002), which considered the Famatina stratigraphy as part of a distal foredeep or forebulge of a single foreland basin.

2. Lower Middle Miocene (Del Abra Formation and Lower Del Buey Formation, MS3)

During the middle Miocene, the upward-fining megasequence MS3 (Fig. 3) was derived from sources to the east. Granite megaboulders, granite-rich blocky conglomerates, and oligomictic composition of sandstones are strong evidence of first-cycle derivation from crystalline sources (Fig. 7). The colluvial deposits at the base of this sequence (Dávila and Astini, 2003a) and clast size are strong evidence of local provenance of a nearby igneous source. Porphyritic granites located to the east of the present Miocene outcrops are most likely the source of the conglomerates. A subtle but noteworthy gradual upsection decrease of subordinate low-grade metamorphic clasts suggests accompanying unroofing of low-grade metamorphic rocks within the progressively uplifted proto–Sierras de Paimán–Ramblones.

Basin Implications

During early middle Miocene deposition of MS3, provenance from the western sources was episodically interrupted, and exhumation of the eastern basement domain began to provide sediment to the basin. The coarse clast size suggests unroofing of porphyritic granites that produced higher gradients and paleoslopes to the west during an intensive deformation phase. Atop of MS3, a stable sedimentation phase dominated, as indicated by deposition in low-gradient environments (playa lakes, lacustrine carbonates, and paleosols). This interpretation is consistent with the highly variable paleocurrents recorded from the upper section of the Del Abra and Del Buey Formations (Fig. 5). Subtle relief during deposition of the Del Buey Formation suggests tectonic quiescence before renewal of contraction in the western domain. Although this interpretation proves basement deformation to the east, the episodic source and facies changes, together with mapped structural and stratigraphic relationships, might relate to half-graben sedimentation (Fig. 8), as a result of localized bending extension (Dávila and Astini, 2003a), instead of an eastward shifting of basement thrusting.

3. Upper Middle Miocene (Upper Del Buey Formation and Santo Domingo Formation, MS4)

The overlying upward-coarsening megasequence MS4 (Fig. 3) reveals a short and rapid change of source area, showing again a marked provenance from the west. An initially stable and relatively flattened relief is supported by development of thick paleosols and extended carbonate lacustrine horizons interbedded within the Del Buey Formation (Dávila, 2005),

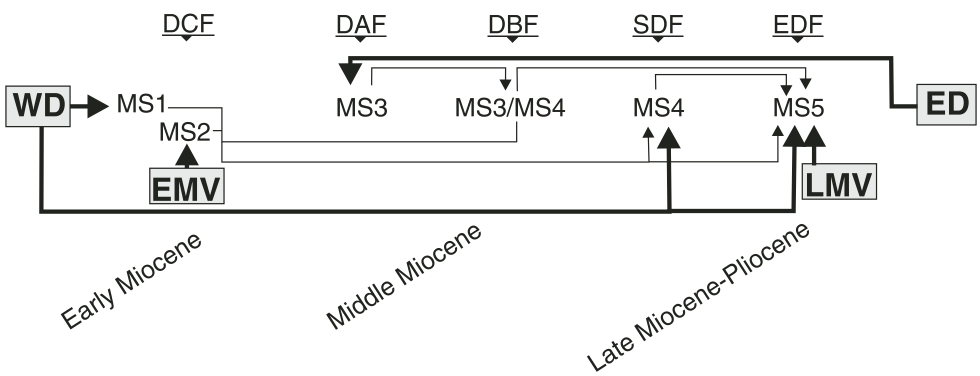

Figure 7. Conglomerate cycling from different source areas. Solid thicker flow lines show first-order provenance, whereas thinner lines depict potential clast recycling from underlying sedimentary units. Primary source areas—western domain (WD, see location in Fig. 2), eastern domain (ED, see location in Fig. 2), early Miocene volcanics (EMV), and late Miocene volcanics (LMV). Cenozoic units were partially cannibalized (see text for details), supplying clasts when exhumed during thrust migration. Note that lower units, Del Crestón Formation and Del Abra Formation, have first-order clasts derived from primary source areas, WD and ED, respectively. DCF—Del Crestón Formation, DAF—Del Abra Formation, DBF—Del Buey Formation, SDF—Santo Domingo Formation, EDF—El Durazno Formation. MS—Megasequences (see text for megasequences and stratigraphic units correlations).

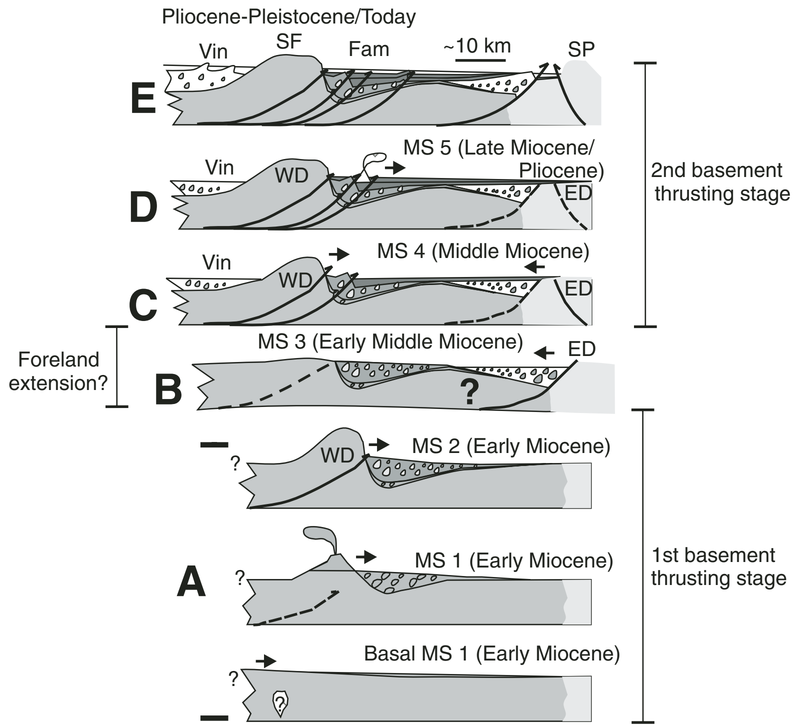

Figure 8. Schematic foreland evolution in Famatina region, southern Central Andes, and suggested megasequences (MS). (A) Early Miocene foreland history: from bottom to top, basal microconglomerate deposition (base of MS1) on a regional planation surface. The rest of MS1 is contemporaneous with andesite volcanism in the retroarc. Granite conglomerate deposition on top of MS2 records basement thrusting and first broken foreland stage, herein inferred to have formed during transition from steep to flat subduction. (B) Early–middle Miocene extensional stage and basin inversion during MS3 formation. (C) Late middle Miocene broken foreland stage during MS4 eolian-fluvial deposition. (D) Late Miocene–Pliocene broken foreland stage and deposition of MS5 with contemporaneous volcanism (dacites). (E) Pleistocene deformation and last structural mountain building. Vin—Vinchina Basin, Fam—Famatina region (study area), SF—Sierra de Famatina, SP—Sierras Pampeanas, WD—western domain (Sierra de Famatina), ED—eastern domain (Sierra de Paimán–Ramblones). See present location in Figure 2.

which is consistent with low-gradient sedimentation and low accumulation rates. Lenticular, rounded, and polymictic fine-grained conglomerates imply recycling from older intrabasinal stratigraphy (Fig. 7), whereas equigranular granite cobbles in the upper Del Buey Formation are clearly derived from the western source domain. The Santo Domingo Formation, with eolian-fluvial interaction, represents the upper part of MS4. Provenance analysis supported by lithofacies analysis indicates that deposition in this eolian-rich section occurred in a relatively proximal alluvial setting surrounded by basement ranges (Dávila and Astini, 2003c). Even though sand composition suggests local provenance, possibly the Cordon de la Cumbre belt (Dávila and Astini, 2003c), only the conglomerate is definitive. Composition analysis on the gravel units, supported by textures and paleocurrent studies, suggests a source area of granite, sedimentary rock, and possibly older Cenozoic conglomerates (andesite conglomerate of the Del Crestón Formation). Composition, together with the lack of porphyritic granite and metamorphic clasts, constrains the western domain as the best candidate for the source of MS4. Although some cobble beds may indicate recycling from lower units, isolated large plutonic boulders reinforce a first-cycle origin for at least part of these strata (Fig. 7).

Basin Implications

Renewed tectonic activity in the western domain (Fig. 3) is suggested by progradation of thick alluvial fans and provenance of upward-coarsening megasequence MS4 (Dávila, 2003, 2005; Dávila and Astini, 2003c). Reactivation of the early Miocene thick-skinned system (Fig. 8) is inferred from the provenance analysis. First-cycle, oversized granite boulders from the top of this megasequence indicate rejuvenation of thrusting of crystalline basement, exposing plutonic bodies in the west. MS1-derived andesite clasts indicate that the early Miocene packages were cannibalized, and, hence, they comprised part of the active and erosional thrust front with an eastward migration of deformation during this episode.

4. Late Miocene–Pliocene (El Durazno Formation, MS5)

The youngest upward-coarsening megasequence MS5 (Fig. 3) reveals similarities to MS4 that match well with the western domain. Compositional data (Appendix 3, see footnote 1) and clast size suggest that first-cycle material (Fig. 3) form the bulk of these conglomerate sheets, but some recycling cannot be discarded, especially of pebbles and granules accompanying the boulder conglomerates (Fig. 7). Composition and paleocurrents indicate a source to the west, from the granitic basement and Paleozoic sedimentary-volcanic pile exposed in the Famatina thrust sheets. The presence of rare limestone clasts (see Appendix 3) suggests that the middle section of the Del Buey Formation (top of MS3 or base of MS4) was cannibalized and converted into a partial source area during MS5 deposition. The Del Buey Formation is the only unit with carbonate rocks in the region. Abundant pumice and porphyritic dacite boulders, analogous to late Miocene–Pliocene volcanism of the region (Mogote Rio Blanco Formation), suggest that these volcanic rocks also contributed to MS5 (Fig. 7). The increase in clast size (Fig. 3) with respect to the underlying sequences implies progressive exhumation of the western domain during deposition.

Basin Implications

In the late Miocene–Pliocene, the conglomerates of the MS5 document ongoing unroofing of western Famatina sources. Deposition of this megasequence (Fig. 3) indicates higher gradients and renewed deformation. An eastward shifting of thrusting is deduced from clast composition, which shows that the early to middle Miocene stratigraphy was locally involved within the thrust system, becoming a source area. The alluvial system shows drainage toward the east and northeast, interacting with volumetrically significant explosive volcanism (Martina et al., 2006), as suggested by interlayered ignimbrite sheets and late Miocene dacite and pumice clasts. It is possible that local relief due to volcanic inflation (i.e., Pritchard and Simons, 2004) and consequent increase of surface gradients allowed deep incision between volcanic and nonvolcanic stages (MS4 and MS5). The unconformity that separates MS5 from MS4 may be related to such volcanically induced phenomena. Foreland sedimentation was, therefore, strongly controlled by volcanism and ongoing basement thrusting (Fig. 8). Our results indicate that MS5 is the only unit that correlates with the late Miocene–Pliocene (7–6.5 Ma) stage of Jordan et al. (2001). Although ages are similar to other broken foreland sections in the westernmost, central, and eastern Sierras Pampeanas (Jordan et al., 2001), contrasting composition suggests no physical connection between dispersal systems.

TECTONIC IMPLICATIONS

In the modern flat-slab segment of the southern Central Andes (28°–33°S), most work suggests that basement deformation and associated broken foreland deposition began ca. 7 Ma (e.g., Jordan et al., 2001; Ramos et al., 2002). Development of broken foreland basins in the Sierras Pampeanas has been closely linked to flat subduction. This tectonic regime is characterized by strong interplate coupling that, together with the stiff rheology of a cool upper lithosphere (e.g., Spencer, 1994), allows deformation to be transferred several hundreds of kilometers cratonward (Gutscher et al., 2000). This condition favors the transmission of compressive stresses well into the distal portion of the foreland. Although a discussion on generation of accommodation space in the Central Andean broken foreland is beyond the scope of this contribution, resulting basement thrusting is the most likely control on basin subsidence (McQueen and Beaumont, 1989; Jordan, 1995), and it is overlapped by the effects of topographic barriers and dynamic topography (Dávila et al., 2005).

As indicated by this study in the northern transition segment from flat-slab to normal subduction in the southern Central Andes, Cenozoic synorogenic megasequences show a protracted broken foreland history from early Miocene onward, likely interrupted by an extensional period possibly associated with localized crustal bending. Farther north of the study region, although early to middle Miocene (20–12 Ma) deformation is poorly constrained, recent work in southern Puna (e.g., Kraemer et al., 1999; P in Fig. 1) and in northern Sierras Pampeanas (e.g., Reynolds et al., 2000; NSP in Fig. 1) indicates a broken distal foreland. This earlier basement partitioning matches the Cenozoic history of Famatina. In contrast, 400 km southward along the boundary between the western Sierras Pampeanas and the Precordillera, the oldest basement uplift is Miocene–Pliocene (e.g., Jordan et al., 2001; Ramos et al., 2002). As a whole, basement deformation in Famatina, northern Sierras Pampeanas, and in the southern Puna (at the present northern transition to normal subduction segment, between 24° and 28°S, depicted TZ in Fig. 1) began in the early–middle Miocene, and later shifted to the east and south to embrace the central and eastern Sierras Pampeanas in the late Miocene (Fig. 9). This propagation of early Miocene basement involvement within the foreland could relate to a shallow-subduction episode, supported in Famatina by the contemporaneous magmatic broadening into the foreland (Dávila et al., 2004b). These observations strengthen the interpretations of eastward and southward migration of the flat-slab segment as subduction continued along the Chile margin. Kay and Mpodozis (2002), based on Yáñez et al. (2001), suggested that the Miocene–Pliocene to modern flat-slab segment is a consequence of southward migration of the Juan Fernandez Ridge. The Juan Fernandez Ridge would have coupled ca. 20 Ma with the Andean margin at the latitudes of the Altiplano (~20°S) and progressively migrated southward (Fig. 9). It is clear that Famatina and the northern Sierras Pampeanas were beyond the influence of the oceanic ridge subduction ca. 17–16 Ma (early–middle Miocene) (Fig. 9). For this reason, we propose that broken foreland development was not coeval along strike and at least the earlier episode was not triggered by subduction of the Juan Fernandez Ridge. It is likely that other changes in coupling parameters (e.g., Gutscher et al., 2000; Yañez and Cembrano, 2004) favored the slab flattening during early Miocene times. An alternative to consider is that an unrecognized branch or independent oceanic plateau, parallel to the Juan Fernandez Ridge,

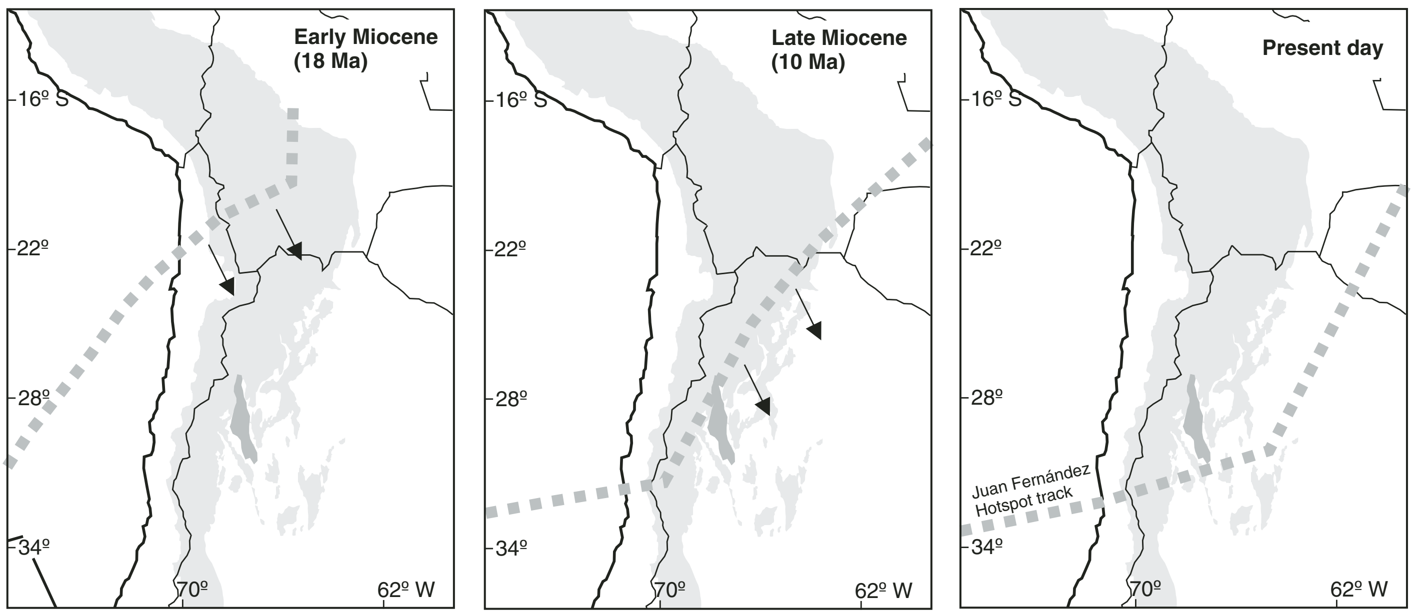

Figure 9. Maps of southern Central Andes showing temporal migration of Juan Fernández Ridge (thick gray dashed line) during Miocene to present (after Yánez et al., 2001; Kay and Mpodozis, 2002). Country borders, continent margin, Famatina Ranges (darker gray area), and Andean belt (lighter gray areas) are shown for reference. Note that Juan Fernandez Ridge subducted beneath the Andean margin near 21°S at 18 Ma, north of modern flat-slab segment (~32°S). Paleogeography is palinspastically unrestored.

collided with the margin of the southern Central Andes since the early Miocene. The migration of such a ridge may additionally explain the flat subduction and related magmatism in the Payunia, southernmost Central Andes (29°–34°S), during the Pliocene (Kay et al., 2004).

Our study in pericratonic areas of South America emphasize aspects to be taken into account in similar tectonic scenarios and in the fossil records. Provenance studies, supported by geochronology and geodynamic modeling, provide a powerful tool to unravel basin dynamics in distant foreland settings where deformation involves crystalline substrates. This allows us to understand exhumation of deep basement roots within the source and to approximate the tectonic load for subsidence analysis. It is also evident that provenance studies help to estimate timing of deformation, paleogeography, and tectonic controls within intraplate settings.

Recurrent stages of basement thrusting and foreland partitioning can occur in intervals <10 m.y. Influence of aseismic ridges may particularly enhance segmentation in the upper plate, triggering basement thrusting into the distal foreland. This is particularly significant for fossil examples where geodynamic setting has to be inferred. Although foreland partitioning may link to flat subduction and increase coupling, from this case in the Central Andes, it is apparent that preexisting fabrics (e.g., stages of intra-orogenic extension; Dávila and Astini, 2003a) played an important control on later broken foreland partitioning.

Present-day intermontane broken foreland landscapes (e.g., Sierras Pampeanas) are not necessarily the result of a single basement trusting stage. Foreland thrusting, for example, can be separated by foreland extension weakening the strong pericratonic foreland and favoring reactivation during later compression.

CONCLUSIONS

Chronostratigraphically constrained provenance analysis on the Tertiary synorogenic sedimentary wedge east of Famatina allows us to understand protracted intermontane-basin formation within the southern Central Andes, and we have contributed new evidence to the wealth of data regarding broken foreland dynamics. The provenance history of strata in the Famatina belt can be summarized in three major unroofing episodes, all of which involved basement deformation from early Miocene to Pliocene (A–B, C, and D–E in Fig. 8). Basement partitioning in the foreland basin began much earlier than has previously been suggested. Along strike in the southern Central Andes, foreland-basement thrusting propagated south and did not fully match southward migration of the Juan Fernandez Ridge. The earliest broken foreland episode developed during the early Miocene and involved the western domain of Famatina, where >4500 m of Paleozoic strata overlie basement. Sedimentation during the early Neogene is represented by a normal unroofing megasequence with superbly preserved rotated unconformities and clear evidence, at the top, of basement involvement within the source. Shortening and initial foreland partitioning was interrupted by shifting of deformation toward the east. This is consistent with exhumation and unroofing of the eastern domain where basement sources predominate to the east of the early Miocene depocenter, as indicated from provenance and inversion of paleocurrents. Renewed shortening in the late middle Miocene and the Miocene–Pliocene contributed to re-exhumation of basement sources to the west and broad reversal of paleocurrents and sources that persisted throughout the late Cenozoic and into the present. Basement uplift interrupted drainage systems and promoted forced aggradation in intermontane depozones. For this reason, synorogenic stratigraphy on both sides of Famatina differs not only in composition, but in preserved thickness.

Our age-controlled provenance analysis in Famatina suggests protracted basement involvement in deformation and incorporates new evidence regarding broken foreland dynamics. Deformation started in early Miocene time between Famatina and northern Sierras Pampeanas, indicating that slab shallowing had started before arrival of the aseismic Juan Fernandez Ridge, which began to control the study region since the Miocene–Pliocene onward.

ACKNOWLEDGMENTS

We appreciate thoughtful revisions by R. Ingersoll and R. Korsch. We thank T. Jordan (Cornell University) for discussions and supporting geochronological analysis. We also acknowledge P. Heller, B. Horton, and C. Garzione, who provided valuable comments on preliminary versions of the manuscript. T. Spell (University of Nevada) supplied the ^{40}Ar-^{39}Ar analytical results. F. Martina and M. Ezpeleta assisted during field work. Argentine science bureaus Secretaría de Ciencia y Tecnología de la Universidad Nacional de Córdoba (SECyT-UNC), Fondo para la Investigación Científica y Tecnológica (FONCyT), and Consejo Nacional de Investigaciones Científicas y Técnicas (CONICET) funded our work.

REFERENCES CITED

Astini, R.A., and Dávila, F.M., 2004, Ordovician retroarc foreland and Ocloyic thrust belt development on the western Gondwana margin as a response to the Precordillera terrane accretion: Tectonics, v. 23, no. 4, p. TC4008, doi: 10.1029/2003TC001620.

Astini, R.A., Dávila, F.M., Collo, G., and Martina, F., 2005, La Formación La Aguadita (Ordovícico Medio-Superior): Su implicancia en la evolución temprana del Famatina y como parte del orógeno oclóyico en el O de Argentina: Revista de la Asociación Geológica Argentina, Publicación Especial 8 (Serie D), p. 67–86.

Barazangi, M., and Isacks, B.I., 1976, Spatial distribution of earthquakes and subduction of the Nazca plate beneath South America: Geology, v. 4, p. 686–692, doi: 10.1130/0091-7613(1976)4<686:SDOEAS>2.0.CO;2.

Barreda, V.D., Ottone, E.G., Dávila, F.M., and Astini, R.A., 2006, Edad y paleoambiente de la Formación del Buey (Mioceno), Sierra de Famatina, La Rioja, Argentina: Evidencias sedimentológicas y palinológicas: Ameghiniana, v. 43, no. 1, p. 215–226.

Beck, R.A., Vondra, C.F., Filkins, J.E., and Olander, J.D., 1988, Syntectonic sedimentation and Laramide basement thrusting, Cordilleran foreland; timing of deformation, *in* Schmidt, C.J., and Perry, W.J., Jr., eds., Interaction of the Rocky Mountain Foreland and the Cordilleran Thrust Belt: Geological Society of America Memoir 171, p. 465–487.

Bossi, G.E., Georgieff, S.M., Gavriloff, I.J.C., Ibañez, L.M., and Muruaga, C.M., 2002, Cenozoic evolution of the intramontane Santa María basin, Pampean Ranges, NW Argentina: Journal of South American Earth Sciences, v. 15, p. 731–734.

Caminos, R., 1979a, Sierras Pampeanas noroccidentales: Salta, Tucumán, Catamarca, La Rioja y San Juan, *in* 2nd Simposio de Geología Regional Argentina: Córdoba, Academia Nacional de Ciencias, v. 1, p. 225–292.

Caminos, R., 1979b, Cordillera Frontal, *in* 2nd Simposio de Geología Regional Argentina: Córdoba, Academia Nacional de Ciencias, v. 1, p. 397–453.

Cardozo, N., and Jordan, T.E., 2001, Causes of spatially variable tectonic subsidence in the Miocene Bermejo foreland basin, Argentina: Basin Research, v. 13, p. 335–357, doi: 10.1046/j.0950-091x.2001.00154.x.

Colombo, F., 1994, Normal and reverse unroofing sequences in syntectonic conglomerates as evidence of progressive basinward deformation: Geology, v. 22, p. 235–238, doi: 10.1130/0091-7613(1994)022<0235:NARUSI>2.3.CO;2.

Dávila, F.M., 2003, Transecta estratigráfica-estructural a los 28°30'–28°54' de Latitud Sur, Sierra de Famatina, provincia de La Rioja, República Argentina [Ph.D. thesis]: Córdoba, Facultad de Ciencias Exactas, Físicas y Naturales, Universidad Nacional de Córdoba, 516 p.

Dávila, F.M., 2005, Revisión estratigráfica del Grupo Angulos (Neógeno) y su implicancia en la evolución del antepaís Andino central, Sierra de Famatina, La Rioja, Argentina: Revista de la Asociación Geológica Argentina, v. 60, no. 1, p. 32–48.

Dávila, F.M., and Astini, R.A., 2002, Geología de la Formación del Crestón, Sierra de Famatina, Argentina: Sedimentación Paleógena en el antepaís Andino?: Revista de la Asociación Geológica Argentina, v. 57, p. 463–482.

Dávila, F.M., and Astini, R.A., 2003a, Early middle Miocene broken foreland development in the southern central Andes: Evidence for extension prior to regional shortening: Basin Research, v. 15, p. 379–396, doi: 10.1046/j.1365-2117.2003.00206.x.

Dávila, F.M., and Astini, R.A., 2003b, Discordancias progresivas en los depósitos pre-Neógenos del Famatina (Formación del Crestón), La Rioja, Argentina y su implicancia en la evolución del antepaís Andino: Revista de la Asociación Geológica Argentina, v. 58, no. 1, p. 109–116.

Dávila, F.M., and Astini, R.A., 2003c, Las eolianitas de la Sierra de Famatina: Interacción paleoclima–tectónica en el antepaís fragmentado Andino central durante el Mioceno Medio?: Revista Geológica de Chile, v. 30, no. 2, p. 187–204.

Dávila, F.M., Astini, R.A., and Schmidt, C.J., 2003, Unravelling 470 my of shortening in the central Andes and documentation of type 0 superposed folding, Famatina Ranges, western Argentina: Geology, v. 31, p. 275–278, doi: 10.1130/0091-7613(2003)031<0275:UMYOSI>2.0.CO;2.

Dávila, F.M., Martina, F., and Astini, R.A., 2004a, Cartografía y cinemática de una rampa lateral en el distrito minero Río Blanco, faja plegada y corrida del borde oriental del Famatina (28°43′S), La Rioja: Revista de la Asociación Geológica Argentina, Serie D, Publicación Especial, v. 7, p. 101–106.

Dávila, F.M., Astini, R.A., Jordan, T.E., and Kay, S.M., 2004b, Early Miocene andesite conglomerates in the Sierra de Famatina, broken foreland region of western Argentina, and documentation of magmatic broadening in the south-central Andes: Journal of South American Earth Sciences, v. 17, p. 89–101, doi: 10.1016/j.jsames.2004.04.001.

Dávila, F.M., Astini, R.A., and Jordan, T.E., 2005, Cargas subcorticales en el antepaís Andino y la planicie pampeana: Evidencias estratigráficas, topográficas y geofísicas: Revista de la Asociación Geológica Argentina, v. 60, p. 775–786.

DeCelles, P.G., 1988, Lithological provenance modelling applied to the Late Cretaceous synorogenic Echo Canyon conglomerate, Utah: A case of multiple source areas: Geology, v. 16, p. 1039–1043, doi: 10.1130/0091-7613(1988)016<1039:LPMATT>2.3.CO;2.

DeCelles, P.G., 1994, Late Cretaceous–Paleocene synorogenic sedimentation and kinematic history of the Sevier thrust belt, northeast Utah and southwest Wyoming: Geological Society of America Bulletin, v. 106, p. 32–56, doi: 10.1130/0016-7606(1994)106<0032:LCPSSA>2.3.CO;2.

DeCelles, P.G., Tolson, R.B., Graham, S.A., Smith, G.A., Ingersoll, R.V., White, J., Schmidt, C.J., Rice, R., Moxon, I., Lemke, L., Handschy, J.W., Follo, M.F., Edwards, D.P., Cavazza, W., Caldwell, M., and Bargar, E., 1987, Laramide thrust-generated alluvial-fan sedimentation, Sphinx conglomerate, southwestern Montana: American Association Petroleum Geologists Bulletin, v. 71, p. 135–155.

DeCelles, P.G., Pile, H.T., and Coogan, J.C., 1993, Kinematic history of the Meade thrust based on provenance of the Bechler conglomerate at Red Mountain, Idaho, Sevier thrust belt: Tectonics, v. 12, p. 1436–1450.

Graham, J., 1988, Collection and analysis of field data, *in* Tucker, M., ed., Techniques in Sedimentology: Oxford, Blackwell Scientific Publications, p. 6–62.

Graham, S.A., Dickinson, W.R., and Ingersoll, R.V., 1975, Himalayan-Bengal model for flysh dispersal in the Appalachian-Ouachita system: Geological Society of America Bulletin, v. 86, p. 273–286, doi: 10.1130/0016-7606(1975)86<273:HMFFDI>2.0.CO;2.

Graham, S.A., Tolson, R.B., DeCelles, P.G., Ingersoll, R.V., Bargar, E., Caldwell, M., Cavazza, W., Edwards, D.P., Follo, M.F., Handschy, J.W., Lemke, L., Moxon, I., Rice, R., Smith, G.A., and White, J., 1986, Provenance modelling as a technique for analysing source terrane evolution and controls on foreland sedimentation, *in* Allen, P.A., and Homewood, P., eds., Foreland Basins: International Association of Sedimentologists Special Publication 8, p. 425–436.

Graham, S.A., Wrafter, J.P., Daly, J.S., and Menuge, J.F., 1991, A local source for the Ordovician Derryveeny Formation, western Ireland: Implications for the Connemara Dalradian, *in* Morton, A.C., Todd, S.P., and Haughton, P.D.W., eds., Development in Sedimentary Provenance Studies: Geological Society of London Special Publication 57, p. 199–213.

Gutscher, M.-A., Spakman, W., Bijwaard, H., and Engdahl, E.R., 2000, Geodynamics of flat subduction; seismicity and tomographic constraints from the Andean margin: Tectonics, v. 19, p. 814–833, doi: 10.1029/1999TC001152.

Haughton, P.D.W., Todd, S.P., and Morton, A.C., 1991, Development in sedimentary provenance studies, *in* Morton, A.C., Todd, S.P., and Haughton, P.D.W., eds., Developments in Sedimentary Provenance Studies: Geological Society of London Special Publication 57, p. 1–11.

Hernández, R.M., Jordan, T.E., Dalenz Farjat, A., Echavarría, L., Idleman, B.D., and Reynolds, J.H., 2005, Age, distribution, tectonics, and eustatic controls of the Paranense and Caribbean marine transgressions in southern Bolivia and Argentina: Journal of South American Earth Sciences, v. 19, p. 495–512, doi: 10.1016/j.jsames.2005.06.007.

Höckenreiner, M., Söllner, F., and Miller, H., 2003, Dating the TIPA shear zone: An Early Devonian boundary between the Famatinian and Pampean systems (NW Argentina): Journal of South American Earth Sciences, v. 16, p. 45–66, doi: 10.1016/S0895-9811(03)00018-X.

Horton, B.K., 1999, Erosional control on the geometry and kinematics of thrust belt development in the central Andes: Tectonics, v. 18, p. 1292–1304, doi: 10.1029/1999TC900051.

Horton, B.K., Hampton, B.A., LaReau, B.N., and Baldellón, E., 2002, Tertiary provenance history of the northern and central Altiplano Plateau (central Andean Bolivia): A detrital record of plateau-margin tectonics: Journal of Sedimentary Research, v. 72, p. 711–726.

Jordan, T.E., 1995, Retroarc foreland basins, *in* Busby, C.J., and Ingersoll, R.V., eds., Tectonics of Sedimentary Basins: Cambridge, Blackwell Science, p. 331–362.

Jordan, T.E., and Allmendinger, R.W., 1986, The Sierras Pampeanas of Argentina: A modern analogue of Rocky Mountain foreland deformation: American Journal of Science, v. 286, p. 737–764.

Jordan, T.E., Schlunegger, F., and Cardozo, N., 2001, Unsteady and spatially variable evolution of the Neogene Andean Bermejo foreland basin, Argentina: Journal of South American Earth Sciences, v. 14, p. 775–798, doi: 10.1016/S0895-9811(01)00072-4.

Kay, S.M., and Mpodozis, C., 2002, Magmatism as a probe to the Neogene shallowing of the Nazca plate beneath the modern Chilean flat-slab: Journal of South American Earth Sciences, v. 15, p. 39–57, doi: 10.1016/S0895-9811(02)00005-6.

Kay, S.M., Gorring, M., and Ramos, V.A., 2004, Magmatic sources, setting and causes of Eocene to Recent Patagonian magmatism (36°S to 52°S latitude): Revista de la Asociación Geológica Argentina, v. 59, p. 556–568.

Kraemer, B., Adelmann, D., Alten, M., Schnurr, W., Erpenstein, K., Kiefer, E., van den Bogaard, P., and Görler, K., 1999, Incorporation of the Paleogene foreland into the Neogene Puna plateau: The Salar de Antofalla area, NW Argentina: Journal of South American Earth Sciences, v. 12, p. 157–182, doi: 10.1016/S0895-9811(99)00012-7.

Lencinas, R., 1994, Los depósitos Pleistocenos–Holocenos del Valle de Famatina, La Rioja, Argentina, *in* 7th Congreso Geológico Chileno: Concepción, Actas, v. 1, p. 465–470.

Martina, F., Dávila, F.M., and Astini, R.A., 2006, Mio-Pliocene volcaniclastic deposits in the Famatina Ranges, southern central Andes: A case of volcanic controls on sedimentation in broken foreland basins: Sedimentary Geology, v. 186, no. 1–2, p. 51–65, doi: 10.1016/j.sedgeo.2005.10.002.

McQueen, H.W.S., and Beaumont, C., 1989, Mechanical models of tilted block basins, *in* Price, R.A., ed., Origin and Evolution of Sedimentary Basins and Their Energy and Mineral Resources: International Union of Geodesy and Geophysics, Geophysical Monograph 48, v. 3, p. 65–71.

Pritchard, M.E., and Simons, M., 2004, Surveying volcanic arcs with satellite radar interferometry: The central Andes, Kamchatka, and beyond: GSA Today, v. 14, no. 8, p. 4–11, doi: 10.1130/1052-5173(2004)014<4:SVAWSR>2.0.CO;2.

Ramos, V.A., Cristallini, E.O., and Pérez, D.J., 2002, The Pampean flat-slab of the central Andes: Journal of South American Earth Sciences, v. 15, p. 59–78, doi: 10.1016/S0895-9811(02)00006-8.

Reynolds, J.H., Galli, C.I., Hernandez, R.M., Idleman, B.D., Kotila, J.M., Hilliard, R.V., and Naeser, C.W., 2000, Middle Miocene tectonic development of the transition zone, Salta Province, northwest Argentina: Magnetic stratigraphy from the Metán Subgroup, Sierra de González: Geological Society of America Bulletin, v. 112, p. 1736–1751, doi: 10.1130/0016-7606(2000)112<1736:MMTDOT>2.0.CO;2.

Schlunegger, F., 1999, Controls of surface erosion of the Alps: Constraints from the stratigraphies of the adjacent foreland basins: International Journal of Earth Sciences, v. 88, p. 285–304, doi: 10.1007/s005310050265.

Spencer, J.E., 1994, A numerical assessment of slab strength during high- and low-angle subduction and implications for Laramide orogenesis: Journal of Geophysical Research, v. 99, p. 9227–9236, doi: 10.1029/94JB00503.

Steidtmann, J.R., and Schmitt, J.G., 1988, Provenance and dispersal of tectogenic sediments in thin-skinned, thrusted terrains, *in* Kleinspehn, K.L., and Paola, C., eds., Basin Analysis: New York, Springer, p. 353–366.

Surlyk, F., 1978, Submarine fan sedimentation along fault scarp on tilted fault blocks (Jurassic-Cretaceous boundary, East Greenland): Grolands Geologiske Undersogelse Bulletin, v. 128, p. 1–108.

Tabbutt, K.D., 1990, Temporal constraints on the tectonic evolution of Sierra de Famatina, northwestern Argentina, using the fission-track method to date tuff interbedded in synorogenic clastic sedimentary strata: The Journal of Geology, v. 98, p. 557–566.

Turner, J.C.M., 1971, Descripción geológica de la Hoja 15d, Famatina (provincias de Catamarca y La Rioja): Buenos Aires, Dirección Nacional de Geología y Minería Boletín, v. 126, p. 106.

Yañez, G., and Cembrano, J., 2004, Role of viscous plate coupling in the late Tertiary Andean tectonics: Journal of Geophysical Research, v. 109, p. B02407, doi: 10.1029/2003JB002494.

Yáñez, G.A., Ranero, C.R., von Huene, R., and Diaz, J., 2001, Magnetic anomaly interpretation across the southern central Andes (32°–34°S): The role of the Juan Fernández Ridge in the late Tertiary evolution of the margin: Journal of Geophysical Research, v. 106, p. 6325–6345, doi: 10.1029/2000JB900337.

Manuscript Received 22 March 2006
Revised Manuscript Received 4 October 2006
Manuscript Accepted 19 October 2006

Printed in the USA